Effect of electric fields on the propagation of ultrasonic pulses in o-TaS_3

M. H. Jericho and A. M. Simpson
Department of Physics, Dalhousie University, Halifax, Nova Scotia, Canada B3H 3J5
(Received 12 December 1985)

We report results on the velocity and attenuation of 10-MHz ultrasonic pulses in o-TaS_3 in the charge-density-wave state and in the presence of electric fields. For applied voltages greater than the threshold voltage for nonlinear conductivity the elasticity was found to decrease and sound absorption to increase. The changes in elasticity are orders of magnitude smaller than those reported for kHz frequencies. A relaxation mechanism for sound absorption is proposed with a relaxation strength and a relaxation time that are functions of temperature as well as of applied voltage. The model further suggests that results of elastic measurements could be strongly sample dependent. A search for a shift in sound velocity as a result of a drifting charge-density wave found an effect an order of magnitude larger than predicted shifts. Possible reasons are discussed.

I. INTRODUCTION

The transition-metal trichalcogenide o-TaS_3 enters a charge-density-wave (CDW) state at the onset temperature $T_0 \sim 220$ K, and as a consequence, the electron energy spectrum in this material shows a gap over most of the Fermi surface. The strongly anisotropic resisitivity increases dramatically at low temperatures. Like $NbSe_3$ at low temperatures, the resistance of TaS_3 becomes non-Ohmic if the measuring voltage exceeds a small threshold value. In one approach, this non-Ohmic behavior is thought to arise from the depinning of the CDW by the applied electric fields and the increase in conductivity is attributed to the extra current carried by the moving CDW condensate. For a detailed review of the extensive experimental and theoretical literature on these materials the reader is referred to the review article by Gruner and Zettl.[1] Recently, Brill and Roark[2] have shown, through elastic measurements at kHz frequencies, that the Young's modulus and the internal friction undergo rapid changes once the threshold voltage that marks the onset of non-Ohmic behavior is exceeded. Similar results were also obtained by Mozurkewich *et al.*[3,4] The exact origin of the softening of the Young's modulus and the corresponding increase in internal friction as the sample enters the non-Ohmic state are not clear at the moment. The assumption of a mobile CDW state in the non-Ohmic regime has led to considerable success in explaining a large variety of experimental results.[1] No direct experimental confirmation of a drifting CDW state in these quasi-one-dimensional materials has been possibile so far, however. A proposal for such a test was made by Coppersmith and Varma,[5] who showed that a longitudinal sound wave traveling in the presence of a moving CDW would have its velocity changed by an amount that is proportional to the CDW drift velocity. They predicted a fractional change in sound velocity $\Delta v/v = 10^{-6}$ for a CDW drifting at 10 cm/s. For specimens normally employed for elastic measurements, such a velocity shift should be easily verifiable.

In order to observe the drifting CDW state directly and to contribute to our understanding of the electric field dependence of the elastic properties, we have studied the propagation characteristics of 10-MHz ultrasonic pulses in o-TaS_3 in the presence of pulsed electric fields. Section II describes the experimental technique, and the results on two TaS_3 samples with different threshold fields are presented in Sec. III. A number of experimental difficulties, particularly in connection with the direct observation of the drifting CDW, are discussed in Sec. IV, and a comparison with the low frequency elastic measurements is made. It is suggested that the various anomalies that have been observed may be a result of a relaxation mechanism that is characterized by a relaxation frequency and a relaxation strength that are dependent on both the temperature and the applied voltage.

II. EXPERIMENTAL PROCEDURE

The samples were prepared by the iodine vapor transport technique from 99.98% pure Ta and 99.9995% pure sulfur. X-ray diffraction results on ground-up samples were consistent with an orthorhombic symmetry. Sample dimensions were about $7 \times 0.015 \times 0.008$ mm^3. The experimental arrangement for sample mounting, shown in Fig. 1, was similar to that described previously.[6] A 10-

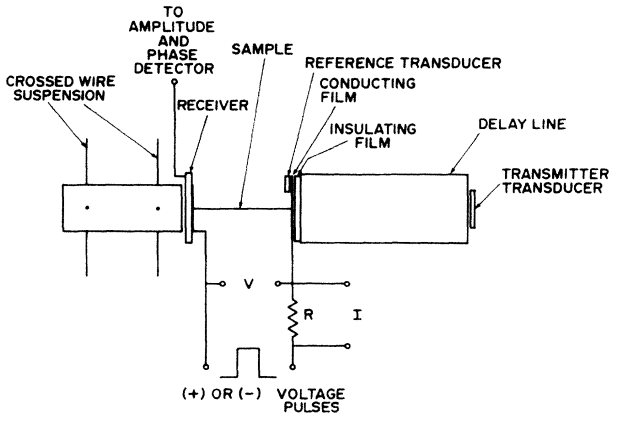

FIG. 1. Experimental arrangement for mounting of ultrasonic transducers and sample.

MHz, 1-μs-wide ultrasonic pulse was launched into the sample every 6 ms from an aluminum delay line and was propagated along the sample length. At this frequency the acoustic wavelength was much larger than the cross-section dimensions of the sample and the fastest acoustic mode has a velocity that is given to a good approximation by $v=\sqrt{E/\rho}$ where E is the Young's modulus. The receiving transducer was coupled to an aluminium cylinder that was constrained to move axially by a crossed-wire suspension. This suspension is elastically very soft and the sample remains essentially stress free during thermal cycling. The launch end of the sample was electrically isolated from the aluminium delay line by a thin insulating film. The sample was acoustically bonded to the delay line and to the receiving transducer with silver paint and conducting epoxy. These acoustic contacts also served as electrical contacts for the electric field measurements. Changes in travel time of an acoustic mode were monitored with a phase comparator. The reference signal for this comparator was obtained from the reference transducer shown in Fig. 1. The phase comparator output went to a Princeton Applied Research (PAR) 164 boxcar averager, and our optimum sensitivity for relative velocity changes of the fastest mode was 5 parts in 10^6 and depended mainly on the quality of the received acoustic signal. The electric field pulses that were applied to the sample could be amplitude swept up to 20 V. In the attempt to observe the effect of a drifting CDW on the sound velocity, electric field pulses of opposite polarity, but of identical shape, were applied alternately to the sample. The two integrator channels of the PAR boxcar then monitored the phase comparator output alternately. The difference between the outputs from the two integrators was displayed on an x-y recorder. The signal-to-noise ratio for this measurement of the velocity difference was somewhat better than in the previous case, and the uncertainty level for the travel time difference for positive and negative field pulses was 5×10^{-12} s, giving an uncertainty for the relative travel time difference $\delta t/t$ of the fastest mode of about 3×10^{-6}. Both the voltage across the sample and the current through it were monitored on a Tektroniks 7600 oscilloscope. In the measurement of the current, the voltage across the resistor R, shown in Fig. 1, was measured with the differential amplifier 7A13. The field pulses had rise and fall times of about 1 μs, and a small ringing effect at the acoustic signal frequency from the rise and fall of the field pulses could be seen at the output of the tuned signal amplifier. For this reason, the leading or trailing edges of the electric field pulses in the experiments, discussed in Sec. III, were not positioned closer than 2 μs to the monitored acoustic pulse.

To obtain information on the amplitude variation of the acoustic signals, the amplitude of rectified signal pulses was monitored with a boxcar integrator and displayed on an x-y recorder simultaneously with the phase measurement.

The sample was surrounded by He exchange gas and temperature was measured with a cryocal diode thermometer. The dc resistance and the differential resistance were measured with standard equipment. The two terminal resistance measurements include the contact resistance to the current leads, which, in our case, was found to be small.

III. RESULTS

A. Voltage and temperature dependence of the field effects

In Fig. 2 the o-TaS_3 samples are characterized by showing the temperature dependence of the electrical resistance, the differential resistance, the threshold field parameter E_T, and the behavior of the extensional wave velocity in zero electric field as a function of temperature. The threshold field parameter, shown in Fig. 2(c), was obtained from the dV/dI curves by the construction shown in Fig. 2(b). For sample 1, in particular, the threshold fields are small, which suggests that the samples were of a reasonable quality.

Figure 3 shows the variation of velocity and mode amplitude for the fastest (extensional) mode in sample 2 as a function of applied voltage. For Fig. 3(a) the 17-μs-wide electric field pulse was placed well ahead of the acoustic signal and electric field effects on the velocity and the amplitude are absent. For Figs. 3(b) and 3(c) the electric field pulse was turned on about 10 μs before the acoustic pulse was launched into the sample and was turned off a few microseconds after the fastest mode had been detected. Both the velocity and the amplitude clearly show a field dependence. The onset of the acoustic anomaly, as shown, for example, in Fig. 3(b) for sample 2, appears to occur at a threshold field of about 2.1 V/cm. The threshold field at that temperature for the onset of non-Ohmic behavior, according to Fig. 2(c), is about 1.3 V/cm, so that the elastic threshold fields appear to be significantly higher than those obtained from electrical measurements. Figures 4(a) and 6 suggest a similar discrepancy for sample 1. The low-frequency Young's modulus measurements,[2-4] on the other hand, showed a very close agreement between the elastic and the conduction threshold fields. In the low-frequency measurements the onset of the elastic anomalies was very sharp and the threshold field could be determined reliably. In our case the onset of the elastic anomaly is generally more gradual and the presence of noise in the traces makes a proper location of the threshold field more difficult. If we use for the location of the elastic threshold field the same construction that was used in Fig. 2(b) for the determination of the electrical threshold field, then we generally find that our threshold fields for velocity and attenuation are higher by about 70% than the electrical threshold fields. The reason for this difference in the results for high and low frequencies is not clear at present. For electric fields that are about twice threshold, the fractional travel time change, $\Delta t/t$, of a 10-MHz extensional mode is at most 2×10^{-4}. This is almost 2 orders of magnitude smaller than the effects reported by Brill *et al.*[2] and about a factor of 20 smaller than the velocity changes reported by Mozurkewich *et al.*[3] The amplitude of the extensional mode decreased with field and did not appear to saturate for fields as high as $5E_T$. The electric field effects on both the velocity and the signal amplitude were more pronounced for acoustic pulses that arrived much later than

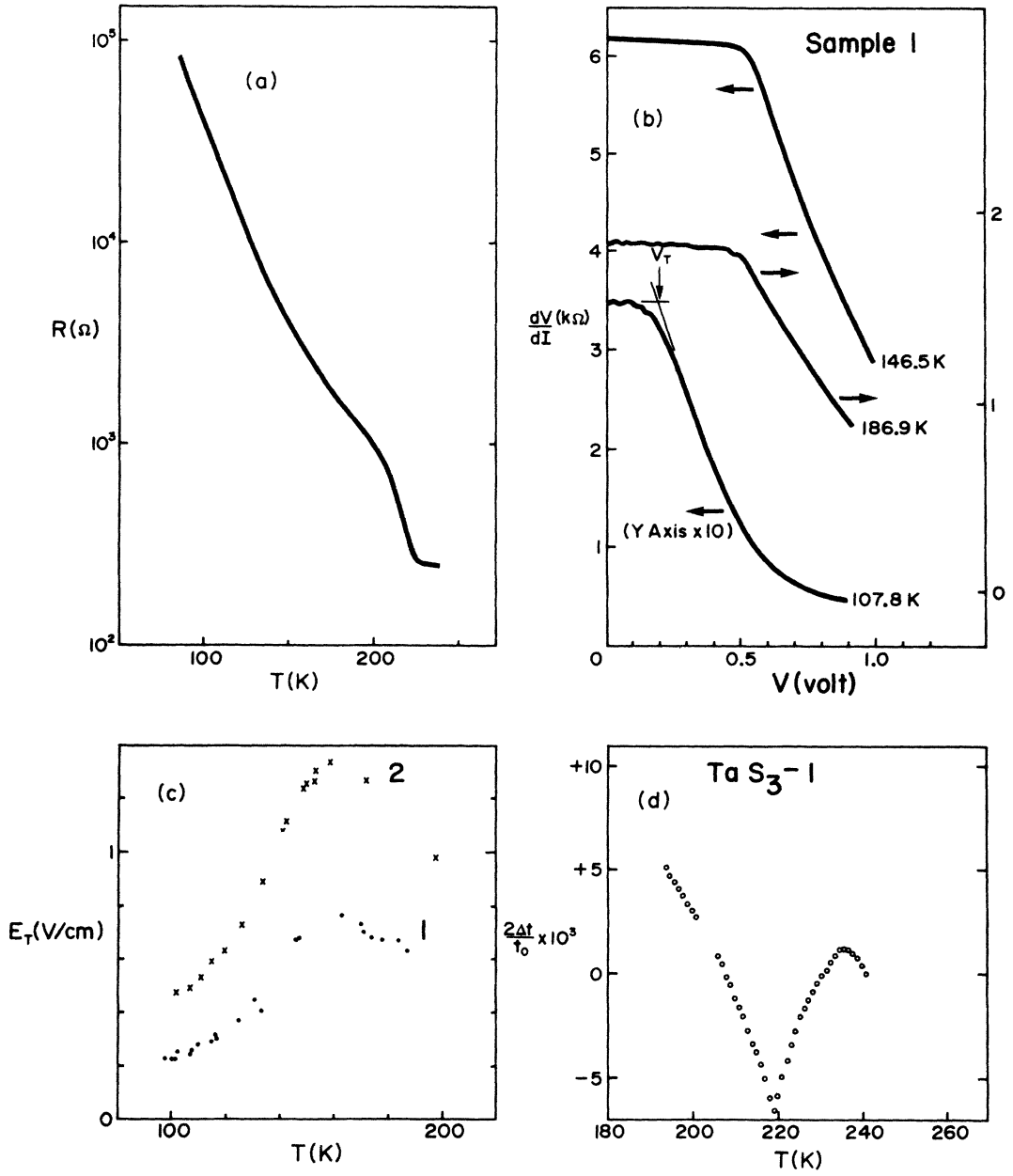

FIG. 2. (a) Resistance versus temperature for sample 2; results for sample 1 were very similar. (b) Differential resistance as function of voltage for sample 1. (c) Threshold fields as function of temperature. (d) Variation of first extensional mode travel time with temperature relative to the travel time at 241 K.

the first transit of the extensional mode. Very similar results were obtained for sample 1. The inset to Fig. 4 shows the variation of Δt for the first extensional mode in sample 1. The threshold voltage for that case is about 0.4 V so that no significant slowing down of this mode was observed for voltages up to at least $4V_T$. For a later arrival, Fig. 4 shows that a significant electric field effect was observed for both the travel time and the signal amplitude. For both samples the electric field effects on the first extensional mode were also studied by applying a dc voltage up to 1.2 V. The results were found to be identical to the pulsed measurements shown in Figs. 3 and 4. The magnitude of the electric field effects was temperature dependent. Near 200 K the effects diminished in amplitude and appeared to saturate after 3 V. Above 240 K (above T_0), electric field effects on all modes were too small to detect for voltages up to 5 V. The effects also diminished at lower temperature.

Figure 5 shows the temperature dependence of the softening at 5 V for the first extensional mode for samples 1 and 2 and the damping of that mode for sample 1. Near the transition temperature, the mode pattern often underwent large changes and reproducible measurements were difficult to obtain. As for sample 2, the electric field effect in sample 1 did not appear to saturate up to at least 10 V. An example of this is shown in Fig. 6, which shows

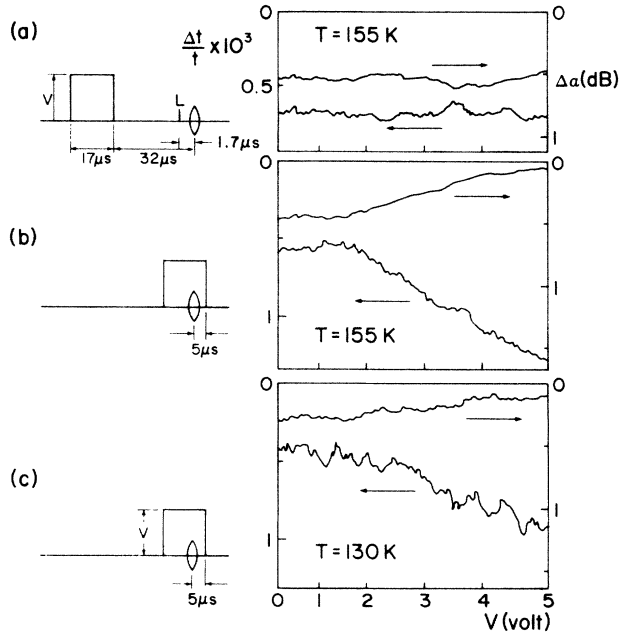

FIG. 3. Fractional changes in velocity and attenuation changes of the first extensional mode in sample 2 as function of voltage for different positions of the voltage pulse. The large noise level in the data does not permit a direct comparison of the elastic threshold fields with those obtained from the electrical measurements. Note the slight nonlinearity of the voltage scale.

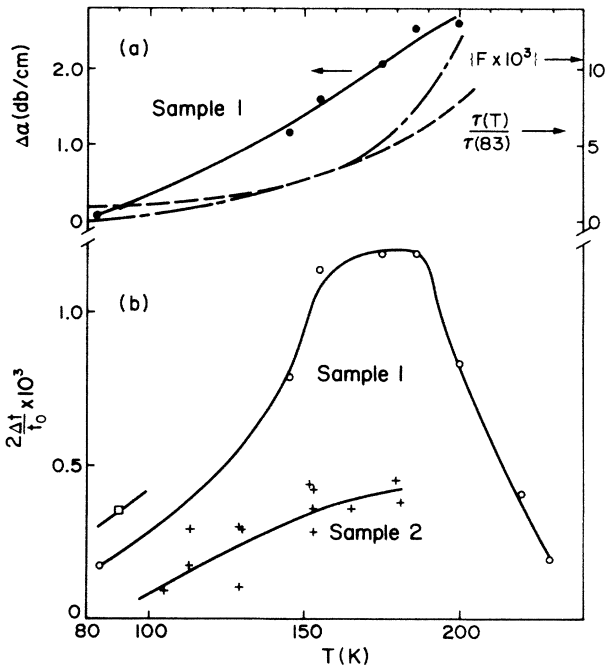

FIG. 5. (a) Solid circles give the temperature dependence of the attenuation increase of the first extensional mode in sample 1 when a 5-V, 40-μs-wide voltage pulse was applied. The dashed line gives the temperature variation of the relaxation time normalized to the value of τ at 83 K. The long-dashed–short-dashed line gives the temperature dependence of the relaxation strength. (b) Corresponding temperature dependence of two times the fractional travel time change in samples 1 and 2. This is equivalent to plotting $\Delta E/E$. All measurements in this figure were made with an electrical history of the samples such that no voltage in excess of 5 V was ever applied. The square marks the value of $2\Delta t/t_0$ obtained with 5 V after high-voltage (20 V) treatment of the sample. All solid lines are an aid to the eye.

the field dependence up to 15 V of the softening of the first extensional mode at low temperatures. The square data point in Fig. 5 represents the softening from Fig. 6 at the 5-V position and clearly lies above the rest of the data. Prior to the measurements shown in Fig. 6 the sample was cycled to voltages near 20 V several times. This treatment always resulted in an increase of the electric field effect for all modes in all samples studied. For the results shown in Figs. 3 to 5 the sample was never cycled past 5 V.

At the larger voltages, effects that seemed to arise from sample heating were noticeable. The travel time of the modes in that case was affected by the position of the field pulse, even if the latter was entirely in advance of the

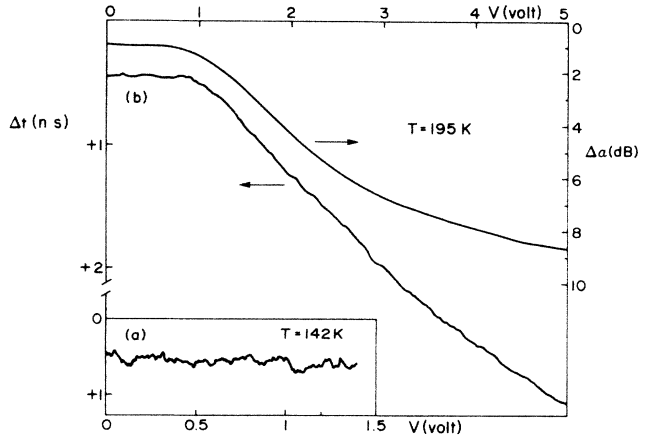

FIG. 4. Voltage dependence of the travel time and amplitude changes of a slow mode (fourth arrival). Inset shows the travel time change for the first extensional mode in the low-voltage regime. All measurements are for sample 1.

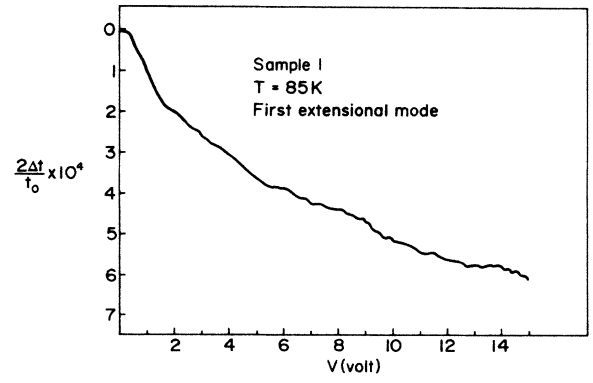

FIG. 6. Fractional slowing down of the first extensional mode in sample 1 at 85 K and for large applied voltages. No clear saturation of the effect is discernable.

acoustic launch time. The velocity shifts induced by such large field pulses varied linearly with the field pulse width and for voltages near 20 V, the amplitude of the voltage pulse decreased towards its trailing edge. Both observations suggest sample heating. Large voltage experiments, near 110 K on sample 2, showed that 20-μs-wide voltage pulses produced heating effects above the noise level for $V > 10$ V. Even if allowance for sample heating was made, however, the field effect on the velocity of the first extensional mode did not reach saturation in this voltage range.

To obtain a more detailed understanding of the phenomenon and to further investigate possible heating effects, we studied in sample 1 the dependence of the amplitude of a mode as a function of the position of the voltage pulse. Results are shown in Fig. 7. In Fig. 7(a), for example, a 50-μs-wide voltage pulse is applied and the amplitude of the mode studied in Fig. 4(b) was investigated. The voltage amplitude was fixed at 5 V, and the time delay τ between the voltage turn on and the launch time of the acoustic pulse was varied. In the region where the voltage pulse is turned on before the acoustic energy is launched into the sample (negative τ region), the amplitude (and travel time) is independent of τ. This was confirmed for τ values as large as -50 μs. As soon as τ goes positive the signal amplitude increased until τ was made longer than the acoustic pulse travel time. The 2-μs-wide region ahead of the acoustic mode arrival time could not be investigated for the reasons mentioned in Sec. II. The fact that, for negative τ values, the acoustic pulse amplitude was independent of the position of the voltage pulse suggests that sample heating is negligible up to at least 5-V pulse amplitudes. In Fig. 7(b) the whole voltage pulse is applied before acoustic energy is launched into the sample. The voltage pulse is then progressively delayed until the acoustic pulse travel period is well within the voltage pulse. Again no change in pulse amplitude (nor travel time) was observed if the voltage pulse was either in advance of the acoustic pulse travel period or when this travel period was completely contained within the voltage pulse. Figure 7(c) shows the variation in the amplitude of the same mode if the voltage pulse is narrowed to about 1.4 μs at half height. The voltage pulse width in this case is somewhat shorter than the transit time of the fastest acoustic mode in the sample. The results for Figs. 7(a) and 7(b) are more or less consistent with an electric field effect that is uniform throughout the sample. That is, the amplitude and phase changes that are observed are not simply a result of the electric field or sample current dependence of insertion losses, nor of phase changes at the transducer sample bonds. The results for Fig. 7(c) are more puzzling, since a more uniform amplitude might be expected when the narrow voltage pulse is advanced within the acoustic mode travel time. This point will be discussed further in Sec. IV.

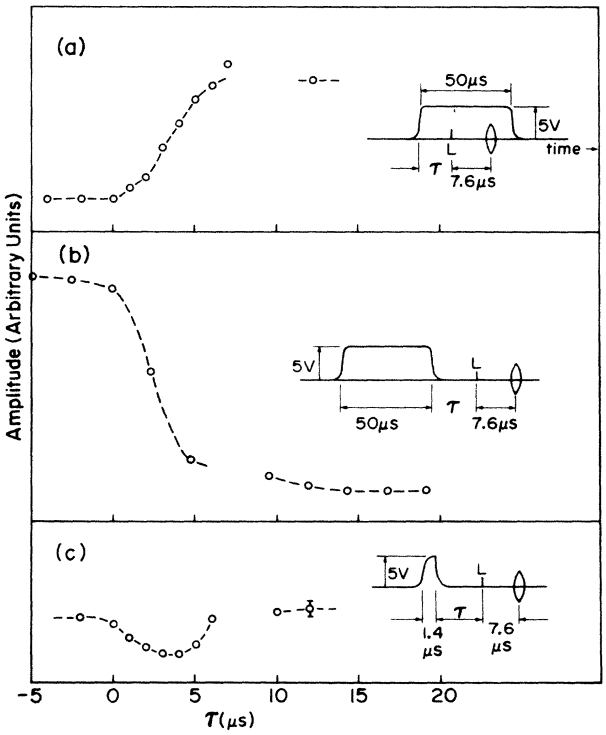

FIG. 7. Variation of the amplitude of a mode that arrived 7.6 μs after acoustic energy was launched into the sample at L. (a) A wide pulse that covers the acoustic pulse travel period is progressively delayed. When the leading edge passes the acoustic launch time the acoustic pulse amplitude rises progressively. (b) Voltage pulse initially well ahead of acoustic launch time. (c) A narrow voltage pulse is progressively delayed and the electric field effect appears less well developed when the voltage pulse is applied close to the receiving time of the acoustic mode.

B. Asymmetry test of the electric field effects

The results for a test of a possible asymmetry in the mode travel time for positive and negative voltage pulses is shown in Fig. 8. The first extensional mode velocity was measured for alternate current pulses as described in Sec. II. For sample 2 the measurements were performed at $T = 126$ K. For large voltage pulses electric field effects on the sound velocity are relatively large in this temperature range. For sample 1 the temperature was lowered to ~ 84 K, a temperature at which the field effects were greatly reduced. The voltage across the sample in this asymmetry test was raised to a maximum of 20 V. As mentioned before, for sample voltages in excess of about 12 V the sample current pulses started to develop a positive slope with only a slight change in the shape of the voltage pulse. For the data on sample 1, at the highest voltages used, the current at the end of the pulse was about 10% larger than at the beginning, although the symmetry between positive and negative pulses was maintained. In this regime the sample current was determined at the position of the acoustic mode that was monitored. The voltage pulses were about 40 μs wide for sample 1 and 10 μs wide for sample 2. The pulse rise and fall portions were positioned well away from the acoustic transit region for the mode under study so that effects from any residual asymmetry in the rise and fall times of the voltage pulses were minimized. In the measurement the pulses were fixed in amplitude and their positions were switched from one that straddled the acoustic mode to

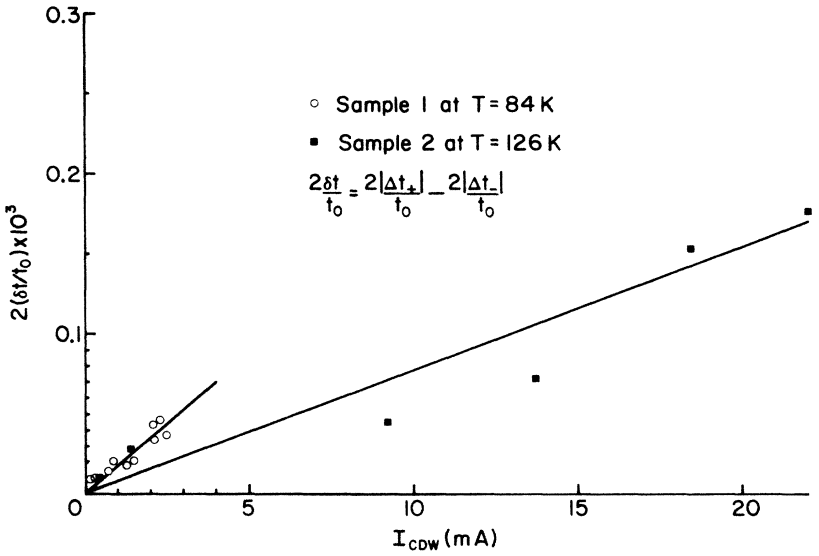

FIG. 8. Difference between the electric field effect for equal amplitude positive and negative current pulses as a function of the CDW current component.

one where voltage turn on occurred after the acoustic mode was detected. For each position the boxcar output was monitored for about 1 to 2 min. on an x-y recorder. In this way the difference in the mode travel time for positive and negative pulses, $\delta t=\Delta t_+ - \Delta t_-$, was determined with a relative error in $\delta t/t$ of 3 parts in 10^6. The small increase in the amplitude of the current within the voltage pulse duration suggests sample heating at very high voltages. Various tests were therefore made to study the effect of sample heating on the boxcar difference signal for the plus and minus voltage pulses. For example, the voltage pulses were deliberately imbalanced and their position was furthermore moved from well ahead of the first acoustic mode to well after its arrival. Such tests carried out for different pulse amplitudes suggested that an imbalance in the pulse power for the two polarities of about 1% (which was the resolution in the present experiment) would contribute, at most, 1 part in 10^6 to the imbalance in travel time. Sample 2 with balanced current pulses also had balanced voltage pulses so that the power was balanced to the above resolution. For sample 1, however, the amplitude of the negative voltage pulses exceed that of the positive pulses by about 0.8 V at the highest voltages, even though the currents were balanced. The resulting power imbalance amounted to 5% for high voltages and probably produced a difference signal from asymmetric heating of about 5 parts in 10^6. The voltage pulse width used for sample 1 was larger than for sample 2. The measurements on sample 1 were made at lower temperature, however, where the Ohmic resistance was considerably larger and heating effects were therefore comparable. The original objective of this test was to examine the possibility of obtaining direct experimental evidence for a drifiting CDW. For this reason the sample currents in this asymmetry test were made identical for positive and negative pulses. The CDW current I_{CDW} was calculated from the relation

$$I_{CDW}=I-V/R_0 ,$$

where I is the total current, V the sample voltage, and R_0 the Ohmic part of the sample resistance.

It is evident from Fig. 8 that both samples show an asymmetry in the electric field effect and an extensional mode is slowed down more if E is antiparallel to the sound propagation direction than when it is parallel.

IV. DISCUSSION

A. Voltage and temperature dependence of the elastic anomalies

The elastic properties of crystals with orthorhombic symmetry are characterized by nine independent elastic constants. In view of this, the mode spectrum of anisotropic elastic waveguides represented by our crystals is very complex. When the sound wavelength is much larger than the lateral sample dimensions, however, the velocity of the fastest extensional mode is expected to be dominated by the Young's modulus along the sample length. In our samples, this modulus then appears little affected by electric fields applied in the CDW state, contrary to the low-frequency results of Brill *et al.*[2] and of Mozurkewich *et al.*[3,4]

It is usually unavoidable that the transmitting transducer couples acoustic energy into a whole spectrum of waveguide modes. The relative amplitude of these modes depends on the nature of the bond between sample and transducer, on transducer tuning, as well as on the temperature. In view of the fact that the elastic properties of o-TaS_3 are not sufficiently well known we were unable to identify slower acoustic pulses with any certainty. It was not possible, for example, to distinguish a flexural from a torsional mode. The results on some of the slower pulses, therefore, represent measurements on unidentified modes.

These slower modes were generally more strongly affected by the electric field than the first extensional mode. If the latter mode, for example, changed by 0.3 dB then a mode positioned at about three times that travel time changed by about 4 dB instead of the 0.9 dB one would have expected if that late arrival had been the second echo of the first extensional mode. It therefore appears that other elastic constants, in addition to the Young's modulus, are affected by the electric field. Shear and torsional modes travel much slower than extensional modes, and it is possible that C_{44} or C_{66} are the elastic constants most affected by the electric field. The interpretation for slow modes is further complicated by mode interference and mode conversion effects. Even in 1-cm-long samples and for pulse widths of less than 1 μs some overlap of modes is unavoidable and the amplitude of a pulse can be affected by interference. The character of a mode can, furthermore, change as a pulse propagates along the sample, due to mode coupling,[7] and it is possible that the measured electric field dependence is influenced by these effects. The results of Fig. 7(c) could be a consequence of mode coupling effects where the mode near the launch end of the sample has a stronger electric-field-dependent character than near the receiver end. Such effects would manifest themselves only through premature flattening of the traces in Figs. 7(a) and 7(b) and our signal-to-noise ratio was not sufficient to draw firm conclusions regarding this effect. Under certain tuning conditions an inspection of the train of acoustic pulses sometimes clearly showed one or two slow modes that were increasing in amplitude when the field was applied, which might suggest that, for slow modes, mode coupling or interference can make a contribution to the electric field effects. In order to avoid complications from the above effects, the measurements shown in Figs. 3 and Fig. 4(a) were performed on the extreme front portion of the first extensional mode. As a consequence, the smaller signal amplitude resulted in poorer signal-to-noise ratio than obtained for the rest of the results. In general, we believe that measurements on the first arrival were not significantly affected by the complications mentioned above.

The response of the acoustic signals to electric fields increased after application of large voltages. In some samples voltages in excess of 12 V often induced an intermittent instability so that the amplitude of the sample current and the voltage across the sample showed erratic jumps. The effect suggested the presence of noisy current contacts. After prolonged application of a high voltage or when the voltages were again reduced to below 12 V, both current and voltage were once more stable but the electric field effects were enhanced (by as much as a factor of 2, in some cases). It is not clear whether this effect is related to the "conditioning" of the sample discussed by Brill *et al.*[2]

It is difficult to draw firm conclusions regarding the interpretation of the electric field effects for the velocity and damping of the ultrasonic modes. The small velocity changes we observed at 10 MHz for the extensional mode when compared to other work at kHz frequencies suggest that the effect is frequency and/or sample dependent.

In our samples the electric-field-induced softening passes through a peak between 150 and 190 K and drops to a small value at low temperatures. This behavior is similar to that reported by Mozurkewich *et al.*[4] for one of their samples. Mozurkewich *et al.*[3] and Brill *et al.*[2] proposed an intrinsic mechanism for the softening of the Young's modulus in the sliding CDW state. If the CDW is pinned, then the CDW and the underlying lattice will distort together as a sound wave is propagated and the CDW provides an extra stiffness for lattice distortions. In the sliding CDW state, however, if the lattice distorts independently of the CDW, a softer elastic constant would be measured. Although the correct order of magnitude of the softening at low frequencies was obtained in their original model, the amount of softening predicted was independent of frequency. Mozurkewich *et al.*[4] later suggested that the origin of the Young's modulus softening might be an electric-field-dependent pinning gap for phase modes.

In the voltage range where sample heating is unimportant, the increase in mode damping with voltage was strongly dependent on temperature, as shown in Fig. 5. The attenuation changes shown are $\Delta\alpha(T)=[\alpha(5\text{ V})-\alpha(0)]$. No clear saturation of the attenuation change had occurred at 5 V ($>10V_T$). This should be compared with the low-frequency results of Brill and Roark,[2] where saturation of the internal friction was clearly seen at higher temperatures. Perhaps a more significant difference between the internal friction results of Ref. 2 and our attenuation results in Fig. 5 is the trend with temperature. The low-frequency internal friction changes increase as the temperature is lowered, while the electric-field-induced changes in the attenuation of 10-MHz extensional modes decreases with temperature over most of the temperature range. Such a behavior can be obtained if a relaxation mechanism is responsible for the damping. If the relaxation time τ increases with decreasing temperature and if it is of such a magnitude that, for the low-frequency experiments $\omega\tau \ll 1$, while for high frequency $\omega\tau \gg 1$, then the high- and low-frequency experiments are carried out on opposite sides of the relaxation peak and the observed reciprocal behavior of the high- and low-frequency damping will result. A relaxation mechanism via CDW domains was originally suggested by Brill *et al.*[2] for the electric-field-induced softening of the Young's modulus.

In the following we explore the consequences of a relaxation model for high- and low-frequency attenuation and modulus changes. For a single relaxation time, τ, the modulus and the internal friction at frequency ω can be written as[8]

$$M = M_u - \frac{M_u - M_R}{1+\omega^2\tau^2}\ , \tag{1}$$

$$Q^{-1} = \frac{M_u - M_R}{\overline{M}} \frac{\omega\tau}{1+\omega^2\tau^2}\ . \tag{2}$$

Here M_u is the very high frequency or unrelaxed modulus, while M_R is the low frequency or relaxed modulus and $\overline{M}=(M_u M_R)^{1/2}$.

We now propose that application of an electric field larger than E_T produces an aggregate of defects in the

sample which results in a softening of M_R. The amount of softening induced may be temperature dependent. At very high frequencies the defects will be unable to respond to the acoustic strain field and M_u is assumed to be voltage independent. The experiments are therefore assumed to measure

$$\frac{\Delta M}{M}=\frac{[M(0,T)-M(V,T)]}{\overline{M}}=\frac{F(V,T)}{f(V,T)}-\frac{F(0,T)}{f(0,T)} \quad (3)$$

and

$$\Delta Q^{-1}=[Q^{-1}(V)-Q^{-1}(0)]$$
$$=F(V,T)\omega\frac{\tau(V,T)}{f(V,T)}-F(0,T)\omega\frac{\tau(0,T)}{f(0,T)} . \quad (4)$$

In these $F(V,T)\equiv[M_u(T)-M_R(V,T)]/\overline{M}$ is the relaxation strength at voltage V and temperature T, and

$$f(V,T)=1+\omega^2\tau^2(V,T) ,$$

where $\tau(V,T)$ is the single relaxation time which may be voltage and temperature dependent. It is now reasonable to assume that for $V<V_T$ any defects that may be present are of a type that will not significantly contribute to the relaxation damping or the modulus change, and we therefore set the relaxation strength $F(0,T)=0$. The application of a voltage in excess of V_T is, on the other hand, assumed to generate defects that can contribute to relaxation with a relaxation time that may be voltage and temperature dependent. Equations (3) and (4) can now be combined so that the relaxation time can be easily calculated from the data via the relation

$$\tau(V,T)=\frac{1}{\omega}\frac{\Delta Q^{-1}}{(\Delta M/M)}=\frac{V_s}{4.35}\frac{\Delta\alpha(\text{dB/cm})}{\omega^2(\Delta M/M)} . \quad (5)$$

For our sample 1 the relaxation time that was determined from Eq. (5) at $V=5$ V is plotted in Fig. 5(a) as the dashed line. The relaxation time is of order 10^{-8} s and increases with temperature. With τ thus determined, the relaxation strength was calculated from Eq. (3) and is shown as the long-dashed—short-dashed line in Fig. 5(a). The relaxation strength, therefore, also increases with temperature in this sample. The temperature dependence of both τ and F is thus responsible for the observed temperature dependence of the modulus softening and the damping. In our model, the increase in F with voltage is thought to arise from an increase in the number of appropriate defects in the sample and it appears that most defects are introduced by the time V reach 3 to 4 times V_T. The small magnitude of the anomalies we observe near threshold makes a determination of τ and F at low voltages difficult. The assumption of a single relaxation time is no doubt an oversimplification, and Eqs. (3) and (4) should be modified to allow for a distribution in τ. A discussion of the results then becomes very difficult and we have, therefore, restricted ourselves here to the single relaxation time approximation.

An analysis of the low-frequency data in Fig. 1 of Ref. 2, using Eq. (5), gives a relaxation time that varies from 9×10^{-5} s to 3×10^{-5} s from 85 to 178 K, respectively. The relaxation time for the sample they investigated thus decreased with increasing temperature and was at least 3 orders of magnitude larger than the relaxation time we obtained for our sample. The relaxation time calculated from Ref. 2 is also voltage dependent. A peculiarity of that data is the saturation of ΔQ^{-1} at higher temperatures, while there is no sign of saturation in the corresponding modulus curves. In the relaxation model saturation of ΔQ^{-1} means that $F(V,T)\tau(V,T)/[1+\omega^2\tau^2(V,T)]$ has become voltage independent so that the voltage dependence of F compensates for the voltage dependence of τ. We suggest that the compensation could be sample dependent. It also does not appear to hold at all temperatures, according to the results of Ref. 2. Saturation of ΔQ^{-1}, furthermore, will not necessarily imply saturation of the modulus change since the two quantities differ by the temperature and field-dependent relaxation time. In the voltage region where the damping saturates, the modulus curves should provide a direct measure of the voltage dependence of τ and the relaxation time should thus decrease with increasing voltage. The relaxation strength for the low-frequency results of Ref. 2 at $(V-V_T)=0.1$ V varies from 5×10^{-3} at 85 K to about 12×10^{-3} at 178 K and increases rapidly with voltage. This magnitude of the relaxation strength in our sample 1 is not reached until voltages near 5 V are applied to the sample.

There seems to be an interesting similarity between the electric-field-induced changes in modulus and damping in o-TaS_3 and the "ΔE" effect in magnetic materials.[9] The latter effect, which is a consequence of the magnetic domain structure in ferromagnetic materials, is strongly dependent on sample quality and sample history. In the ΔE effect an applied magnetic field removes domains until in the magnetically saturated state the unrelaxed modulus is obtained. In o-TaS_3, on the other hand, we suggest that application of an electric field in excess of E_T creates defects that soften the modulus and increase the damping via a relaxation process. Impurities might affect the response of such defects to elastic strain, and the dependence of experimental results on sample quality and history is therefore not surprising. The nature of the electric-field-induced defects and hence the microscopic origin of the relaxation is not clear at present. It is possible that domains, as discussed previously,[2] or perhaps metastable-phase pinned CDW states[10–12] play a role in determining the elastic response of TaS_3, although such states are generally only considered for voltages below or only slightly above threshold. If a relaxation process for the damping of elastic waves is created in the non-Ohmic regime than a voltage and temperature dependent relaxation strength, as well as relaxation time, is obtained from experimental data via Eqs. (3) and (4) without making further assumptions. The strong voltage dependence of the relaxation strength can be understood simply as resulting from an increase in the defect concentration with field. The voltage dependence of the relaxation time, on the other hand, is more difficult to understand but perhaps suggests that metastable CDW states with field-dependent activation energies are involved.

B. Asymmetry test of the electric field effects

The electric field effects we observe for low voltages are much smaller than those reported previously at low fre-

quency. Nevertheless, the change in acoustic mode travel time, even for fields that are only a few times the threshold field, is much larger than the interaction effects discussed by Coppersmith and Varma.[5] Their calculation suggests that the shift in the sound velocity, Δv_s, when the CDW condensate drifts with velocity $v_{\rm CDW}$ parallel to the sound propagation direction is given by

$$\Delta v_s = |\delta|^2 Q^2 v_{\rm CDW} , \quad (6)$$

where $|\delta|^2$ is the amplitude of the CDW distortion and Q is the CDW wave vector. In our experiment with alternating positive and negative voltage pulses, the above effect should be doubled. For an estimate of the expected shift, we let $Q_{\rm CDW}=(2\pi/C)$, $|\delta|=0.05$,[5] $v_s=4\times10^3$ m/s (for our first arrival), and $v_{\rm CDW}=J_{\rm CDW}/ne$, where we assumed $n=6.5\times10^{27}$ carriers/m^3.[1]

For sample 2 the asymmetry in the electric field effect was investigated near $T=125$ K. In this temperature region current densities near 2.5×10^8 A/m^2 could be obtained so that the maximum CDW drift velocity was about 24 cm/s. As is clear from Fig. 8, the observed asymmetry is about a factor of 30 larger than the effect predicted by Coppersmith and Varma.[5] In the high-voltage region, sample heating was noticeable, as mentioned in Sec. III. As discussed there, the observed asymmetry is not, however, a result of asymmetric heating of the sample by the field pulses. For sample 2, for example, for identical currents, the voltages for both polarities were also identical up to the maximum voltages used, so that heating effects should have been sufficiently symmetrical. For sample 1 the asymmetry test was carried out at a much lower temperature in order to minimize the single polarity electric field effect. The travel time increase for the first arrival for a 1.47-mA sample current and for $V\sim80V_T$ is only ~0.5 ns, so that the fractional change in velocity at the lowest temperature is only about 0.03%. In view of the much larger sample resistance at low temperatures, the maximum current was limited to about 2.5 mA. An asymetry in the travel time for positive and negative field pulses was, nevertheless, detectable and, as explained in the preceding section, only a part of this might result from asymmetric sample heating. The observed asymmetry is too large to be identified as the Coppersmith-Varma effect. It is more likely that the observed difference signal is a result of a small asymmetry in the single polarity electric field effect. Hysteresis effects in the electrical properties of TaS_3 and other quasi-one-dimensional materials are well known and have been studied extensively.[13–17] Hysteresis is observed in the low-field normal-state resistivity as well as for fields above threshold when the polarity of voltage pulses applied to the sample is reversed.[13,16,17] The latter effect has been attributed to the establishment of a nonuniform CDW state in the sample where $\mathbf{q}$, the CDW wave vector, varies from one end of the sample to the other. When the polarity of the electric field pulse is reversed, the gradient of $\mathbf{q}$ also reverses and various relaxation effects of these polarized states have been studied. In these models the hysteresis of the normal resistance is attributed to metastable CDW states. Ong *et al.*[17] discuss the hysteresis effects in terms of two pristine CDW states. With the sample placed in one of these states through the application of a given current, the alternate state can be obtained if the current direction is reversed. Transformation from one pristine state to the other takes place with a characteristic time $t_0\sim\exp(A/VT)$, where A is a constant and V is the applied voltage.

In our asymmetry test the difference in the acoustic pulse travel time for alternate polarity current pulses was measured. With the current pulses turned off and the sample therefore in one of the pristine states (or in a mixture of the two), the boxcar integrator outputs were zeroed. With the current pulses applied, the difference in the two integrator signals was recorded as described in Sec. II. The difference signal should then be sensitive only to differences in the sound velocities when the alternate polarity pulses are applied. For voltages below threshold, conversion times t_0 between the two stable CDW states can be long. For voltages of several volts (as used in the asymmetry test), the results of Ref. 17 suggest $t_0<0.5$ μs and conversion should be nearly complete when the sound velocity is measured. The observed asymmetry signal may then represent some residual asymmetry in the two sliding CDW states, but it is difficult to speculate about the detailed nature of these states from the data. An unambiguous direct demonstration of a drifting CDW state will therefore require a resolution of a few parts in 10^7 for relative velocity changes and, more importantly, will require a situation where the first-order electric field effect and the asymmetry in this effect is essentially absent.

V. SUMMARY

We have examined the velocity and damping of 10-MHz ultrasonic waveguide modes in o-TaS_3 in the non-Ohmic regime. Extensional modes have their modulus softened and their attenuation increased when the voltage exceeds the threshold value. The observed changes are, however, orders of magnitude smaller than those reported at lower frequencies. The effect of electric fields is more pronounced on slower moving modes, and it is suggested that at 10 MHz shear or torsional elastic constants might be more strongly field dependent than the Young's modulus. Over most of the temperature range no clear saturation of the electric field effects in either the velocity or the damping was evident for fields in excess of $10E_T$. The electric-field-induced softening of extensional modes we observed is temperature dependent and passes through a maximum between 160 and 190 K, while the corresponding changes in the damping decrease strongly below 200 K. The magnitude of these effects also depends on the electric history of the samples, and the effects generally increased after application of a large voltage in excess of 12 V. A small (at the part in 10^5 level) asymmetry in the electric-field-induced softening was also observed when a succession of electric field pulses of alternate polarity was applied. The observed asymmetry was, however, about an order of magnitude larger than that expected from a drifting CDW and may be related to the hysteresis effects reported for TaS_3.

We have proposed a relaxation mechanism for the electric-field-induced changes in the elastic properties of TaS_3. Comparison of the available experimental data with such a model suggests that the relaxation strength and the relaxation time are both a function of temperature and of electric field, and that both can vary substantially from sample to sample. The exact origin of the relaxation mechanism is not clear at present, but it is suggested that metastable CDW states, or, alternatively, CDW domains may be responsible for the relaxation.

ACKNOWLEDGMENTS

We would like to thank B. Fullerton for the preparation of the samples. This work was carried out with the help of a grant from the Natural Sciences and Engineering Research Council of Canada.

[1]G. Gruner and A. Zettl, Phys. Rep. **119**, 117 (1985).

[2]J. W. Brill and W. Roark, Phys. Rev. Lett. **53**, 846 (1984); in *Charge Density Waves in Solids,* edited by Gy. Hutiary and J. Solyom (Springer-Verlag, New York, 1984), p. 347.

[3]G. Mozurkewich, P. M. Chaikin, W. G. Clark, and G. Gruner, in *Charge Density Waves in Solids,* edited by Gy. Hutiray and J. Solyom (Springer-Verlag, New York, 1984), p. 353.

[4]G. Mozurkewich, P. M. Chaikin, W. G. Clark, and G. Gruner, Solid State Commun. **56**, 421 (1985).

[5]S. N. Coppersmith and C. M. Varma, Phys. Rev. B **30**, 3566 (1984).

[6]M. H. Jericho, A. M. Simpson, and R. Frindt, Phys. Rev. B **18**, 5842 (1978).

[7]T. R. Meeker and A. H. Meitzler, in *Physical Acoustics,* edited by W. P. Mason (Academic, New York, 1984).

[8]C. Zener, *Elasticity and Anelasticity of Metals* (University of Chicago Press, Chicago, 1952).

[9]W. P. Mason, *Physical Acoustics and the Properties of Solids* (Van Nostrand, New York, 1958).

[10]P. B. Littlewood and T. M. Rice, Phys. Rev. Lett. **48**, 44 (1982).

[11]H. Matsukawa and H. Takayama, Solid State Commun. **50**, 283 (1984).

[12]S. Abe, J. Phys. Soc. Jpn. **54**, 3494 (1985).

[13]A. W. Higgs and J. C. Gill, Solid State Commun. **47**, 737 (1983).

[14]Gy. Hutiray, G. Mihaly, and L. Mihaly, Solid State Commun. **47**, 121 (1983).

[15]G. Mihaly and L. Mihaly, Phys. Rev. Lett. **52**, 149 (1984).

[16]G. Mihaly, G. Kriza, and A. Janossy, Phys. Rev. B **30**, 3578 (1984).

[17]N. P. Ong, D. D. Duggan, C. B. Kalem, and T. W. Jing, in *Charge Density Waves in Solids,* edited by Gy. Hutiray and J. Solyom (Springer-Verlag, New York, 1984), p. 387.